Hindawi Publishing Corporation
Mathematical Problems in Engineering
Volume 2014, Article ID 606843, 11 pages
http://dx.doi.org/10.1155/2014/606843

Research Article

Symbol Error Rate for Nonblind Adaptive Equalizers Applicable for the SIMO and FGn Case

Monika Pinchas

Department of Electrical and Electronic Engineering, Ariel University, 40700 Ariel, Israel

Correspondence should be addressed to Monika Pinchas; monika.pinchas@gmail.com

Received 1 December 2013; Revised 5 February 2014; Accepted 6 February 2014; Published 11 March 2014

Academic Editor: Kue-Hong Chen

A nonzero residual intersymbol interference (ISI) causes the symbol error rate (SER) to increase where the achievable SER may not answer any more on the system's requirements. Recently, a closed-form approximated expression was derived by the same author for the residual ISI obtained by nonblind adaptive equalizers for the single-input single-output (SISO) case. Up to now, there does not exist a closed-form expression for the residual ISI obtained by nonblind adaptive equalizers for the single-input multiple-output (SIMO) case. Furthermore, there does not exist a closed-form expression for the SER valid for the SISO or SIMO case that takes into account the residual ISI obtained by nonblind adaptive equalizers and is valid for fractional Gaussian noise (fGn) input where the Hurst exponent is in the region of $0.5 \leq H < 1$. In this paper, we derive a closed-form approximated expression for the residual ISI obtained by nonblind adaptive equalizers for the SIMO case (where SISO is a special case of SIMO), valid for fGn input where the Hurst exponent is in the region of $0.5 \leq H < 1$. Based on this new expression for the residual ISI, a closed-form approximated expression is obtained for the SER valid for the SIMO and fGn case.

1. Introduction

We consider a nonblind deconvolution problem in which we observe the multiple output of a finite impulse-response (FIR) single-input multiple-output (SIMO) channel (unknown channel) from which we want to recover its input using adjustable linear filters (equalizers) and training symbols. In the field of communication, SIMO channels appear either when the signal is oversampled at the receiver or from the use of an array of antennas in the receiver [1–6]. It should be pointed out that, for the SIMO case, the same information is transmitted through different subchannels and all received sequences will be distinctly distorted versions of the same message, which accounts for a certain signal diversity [6, 7]. Therefore, it is reasonable to assume that more information about the transmitted signal will be available at the receiver end [6, 7]. SIMO transmission is widely replacing single-input single-output (SISO) approach to enhance the performance via diversity combining [6, 8]. It is well known that ISI is a limiting factor in many communication environments where it causes an irreducible degradation of the bit error rate (BER) and SER, thus imposing an upper limit on the data symbol rate [1, 6]. In order to overcome the ISI problem, an equalizer is implemented in those systems [6]. For the blind SIMO channel equalization case, we may find the following methods [9–13] which exploit various properties of the input signal.

In this paper we consider the nonblind adaptive equalizer where training sequences are needed to generate the error that is fed into the adaptive mechanism which updates the equalizer's taps [14–17]. The nonblind adaptive approach yields in most cases better equalization performance considering convergence speed and equalization quality compared with the blind adaptive version [18]. In addition, the blind adaptive version has a higher computational cost compared to its nonblind approach [18].

Recently [19], a closed-form approximated expression (or an upper limit) was derived for the residual ISI obtained by nonblind adaptive equalizers for the SISO case that depends on the stepsize parameter, equalizer's tap length, input signal statistics, signal-to-noise ratio (SNR), and channel power and is valid for the fGn case where the Hurst exponent is in the region of $0.5 \leq H < 1$. But this expression is not valid for the SIMO case. Thus, there is still no answer on the question

of how the number of receiving antennas contributes to the residual ISI obtained by nonblind adaptive equalizers in the convergence region for the fGn input case with $0.5 \leq H < 1$. Since up to now there does not exist a closed-form expression for the residual ISI obtained by nonblind adaptive equalizers for the SIMO case, no closed-form expression exists either for the SER valid for the SIMO case that takes into account the residual ISI.

In this paper, we propose a closed-form approximated expression for the residual ISI obtained by nonblind adaptive equalizers for the SIMO case (where SISO is a special case of SIMO). This new expression depends on the stepsize parameter, equalizer's tap length, input signal statistics, SNR, channel power, and the number of receiving antennas and is valid for the fGn case where the Hurst exponent is in the region of $0.5 \leq H < 1$. Please note that $H = 1$ is the limit case, which does not have much practical sense [20–22]. It should be pointed out that a white Gaussian process is a special case ($H = 0.5$) of the fGn model [23]. FGn with $H \in (0.5, 1)$ corresponds to the case of long-range dependency (LRD) [23]. Thus, the new obtained expression for the achievable residual ISI is not only valid for the special case of white Gaussian process but covers also those cases that correspond to the case of LRD. The Hurst exponent H may be estimated with the rescaled range (R/S) method [24, 25]. Based on the new proposed expression for the residual ISI, a closed-form approximated expression is obtained for the SER valid for the SIMO and fGn case where nonblind adaptive equalizers are used in the system.

The paper is organized as follows. After having described the system under consideration in Section 2, the closed-form approximated expressions for the residual ISI and SER are introduced in Section 3. In Section 4 simulation results are presented and the conclusion is given in Section 5.

2. System Description

The system under consideration, illustrated in Figure 1, is the same system described in [6]. In this paper, we make the following assumptions as done in [6].

(1) The source sequence $x[n]$ belongs to a real or two independent quadrature carrier case constellation inputs with variance σ_x^2 where $x_r[n]$ and $x_i[n]$ are the real and imaginary parts of $[n]$, respectively.

(2) The unknown subchannel $h^{(m)}[n]$ ($m = 1, 2, 3, \ldots, M$ where M is the number of subchannels) is a possibly nonminimum phase linear time-invariant filter. There is no common zero among all the subchannels. There are M subchannels since there are M receiving antennas.

(3) Each equalizer $c^{(m)}[n]$ ($m = 1, 2, 3, \ldots, M$) is a tap-delay line.

(4) The noise $w^{(m)}[n]$ ($m = 1, 2, 3, \ldots, M$) consists of $w^{(m)}[n] = w_r^{(m)}[n] + jw_i^{(m)}[n]$ where $w_r^{(m)}[n]$ and $w_i^{(m)}[n]$ are the real and imaginary parts of $w^{(m)}[n]$, respectively, and $w_r^{(m)}[n]$ and $w_i^{(m)}[n]$ are independent. Both $w_r^{(m)}[n]$ and $w_i^{(m)}[n]$ are fractional Gaussian noises (fGn) with zero mean.

For $m = k$ we have

$$E\left[w_r^{(m)}[n]\, w_r^{(k)}[\widetilde{n}]\right] = \sigma_{w_r}^2 \delta[n - \widetilde{n}],$$
$$E\left[w_i^{(m)}[n]\, w_i^{(k)}[\widetilde{n}]\right] = \sigma_{w_i}^2 \delta[n - \widetilde{n}]. \tag{1}$$

For $m \neq k$ we have

$$\begin{aligned} &E\left[w_r^{(m)}[n]\, w_r^{(k)}[\widetilde{n}]\right] \\ &= \frac{\sigma_{w_r}^2}{2}\left[(|m-k|-1)^{2H} - 2(|m-k|)^{2H} + (|m-k|+1)^{2H}\right] \\ &\quad \times \delta[n - \widetilde{n}], \\ &E\left[w_i^{(m)}[n]\, w_i^{(k)}[\widetilde{n}]\right] \\ &= \frac{\sigma_{w_i}^2}{2}\left[(|m-k|-1)^{2H} - 2(|m-k|)^{2H} + (|m-k|+1)^{2H}\right] \\ &\quad \times \delta[n - \widetilde{n}], \end{aligned} \tag{2}$$

where $E[\cdot]$ denotes the expectation operator on $(\cdot)$, δ is the Kronecker delta function, and H is the Hurst exponent. In the following, we assume that $\sigma_{w_i}^2 = \sigma_{w_r}^2$ and $\sigma_w^2 = \sigma_{w_i}^2 + \sigma_{w_r}^2$.

According to Figure 1, the mth observation $y^{(m)}[n]$ ($y^{(m)}[n] = x[n] * h^{(m)}[n] + w^{(m)}[n]$) is the result of a linear convolution between the source signal $x[n]$ and the corresponding channel response $h^{(m)}[n]$, corrupted by noise $w^{(m)}[n]$, where "$*$" denotes the convolution operation. The equalizer's output $z[n]$ is derived as follows:

$$\begin{aligned} z[n] &= \sum_{m=1}^{m=M} z^{(m)}[n] = \sum_{m=1}^{m=M} y^{(m)}[n] * c^{(m)}[n] \\ &= \sum_{m=1}^{m=M} \left(x[n] * h^{(m)}[n] * c^{(m)}[n] + w^{(m)}[n] * c^{(m)}[n]\right) \\ &= x[n] + p[n] + \widetilde{w}[n], \end{aligned} \tag{3}$$

where $p[n]$ is the convolutional noise ($p[n] = x[n] * \xi[n]$), $\xi[n] = \sum_{m=1}^{m=M} h^{(m)}[n] * c^{(m)}[n] - \delta[n]$, and $\widetilde{w}[n] = \sum_{m=1}^{m=M} w^{(m)}[n] * c^{(m)}[n]$. Next we turn to the adaptation mechanism of the equalizer in each subchannel which is based on training symbols [14–17, 26]

$$\begin{aligned} \underline{c}^{(m)}[n+1] &= \underline{c}^{(m)}[n] - \mu^{(m)}(z[n] - x[n])\, \underline{y}^{(m)*}[n] \\ &= \underline{c}^{(m)}[n] - \mu^{(m)} P[z[n]]\, \underline{y}^{(m)*}[n], \end{aligned} \tag{4}$$

where $\mu^{(m)}$ is the stepsize parameter in the subchannel, $P[z[n]] = z[n] - x[n]$, $\underline{c}^{(m)}[n]$ is the equalizer vector where the input vector is $\underline{y}^{(m)}[n] = [y^{(m)}[n] \cdots y^{(m)}[n-N+1]]^T$, and N is the equalizer's tap length. The operators $(\cdot)^T$ and $(\cdot)^*$ denote for transpose and conjugate of the function $(\cdot)$, respectively.

3. Residual ISI and SER for the SIMO and Fractional Gaussian Noise Case

In this section, a closed-form approximated expression is derived for the residual ISI valid for the SIMO and fGn case. Based on this new expression, the SER is obtained.

3.1. Derivation of the Residual ISI. In this subsection we derive the residual ISI valid for the SIMO and fGn case.

Theorem 1. *For the following assumptions:*

(1) *the convolutional noise, $p[n]$, is a zero mean, white Gaussian process with variance $\sigma_p^2 = E[p[n]p^*[n]]$. The real part of $p[n]$ is denoted as $p_r[n]$ and $E[p_r^2[n]] = m_p$;*

(2) *the source signal $x[n]$ is a square QAM (quadrature amplitude modulation) signal (where the real part of $x[n]$ is independent with the imaginary part of $x[n]$) with known variance and higher moments;*

(3) *the convolutional noise $p[n]$ and the source signal are independent;*

(4) *the gain between the source and equalized output signal is equal to one;*

(5) *the convolutional noise $p[n]$ is independent with $\widetilde{w}[n]$;*

(6) *the added noise is fGn as defined in the previous section in assumption* (4)*;*

(7) *the Hurst exponent is in the range of* $0.5 \le H < 1$,

the residual ISI expressed in [dB] units may be defined as

$$\mathrm{ISI} = 10\log_{10}\left(m_p\right) - 10\log_{10}\left(\sigma_{x_r}^2\right), \tag{5}$$

where

$$m_p = \frac{\sigma_{\widetilde{w}_r}^2 N\sigma_x^2 \sum_{m=1}^{m=M} \mu^{(m)} \left(\sum_{k=0}^{k=R-1} \left|h_k^{(m)}[n]\right|^2 + (1/\mathrm{SNR})\right)}{2 - N\sigma_x^2 \sum_{m=1}^{m=M} \mu^{(m)} \left(\sum_{k=0}^{k=R-1} \left|h_k^{(m)}[n]\right|^2 + (1/\mathrm{SNR})\right)} \tag{6}$$

with

$$\sigma_{\widetilde{w}_r}^2 \cong \sum_{m=1}^{M} \frac{\sigma_{x_r}^2}{M^2 \mathrm{SNR} \sum_{k=0}^{k=R-1} \left|h_k^{(m)}[n]\right|^2} \times \left(1 + H\left(2H-1\right)\left(M-1\right)\right), \tag{7}$$

where $\mathrm{SNR} = \sigma_x^2/\sigma_w^2$ and $\sigma_{x_r}^2$ is the variance of $x_r[n]$.

Comments. It should be pointed out that assumptions (1)–(7) from above are precisely the same assumptions made in [6]. In addition, assumptions (1), (3), and (5) were also used in [18, 27–33] where [31] explained why assumptions (1) and (3) can hold for the latter stages of the deconvolution process for which our residual ISI is derived. Since the noise and the source signal are independent in practical applications, assumption (5) holds. For a square QAM constellation, the real and imaginary parts of the constellation input are always independent and, in practical applications, the update mechanism of the equalizer is given by (4) where the gain between the equalized output signal $z[n]$ and the source signal $x[n]$ is equal to one. Thus, assumptions (2) and (4) are reasonable and are met in practical applications. FGn gains wide applications in various fields, ranging from geosciences to telecommunications [34]. FGn is a commonly used model of network traffic with LRD [35]. This traffic may for instance play as an interferer on other communication links. Thus, assumptions (6) and (7) are also reasonable and can be met in practical applications.

Proof. The real part of $\widetilde{w}[n]$, namely, $\widetilde{w}_r[n]$, may be expressed as

$$\widetilde{w}_r[n] = \sum_{m=1}^{M} \sum_{k=0}^{k=N-1} \left(c_r^{(m)}[k]\, w_r^{(m)}[n-k] - c_i^{(m)}[k]\, w_i^{(m)}[n-k]\right), \tag{8}$$

where $c_r^{(m)}[k]$ and $c_i^{(m)}[k]$ are the real and imaginary parts of $c^{(m)}[k]$, respectively. The variance of $\widetilde{w}_r[n]$ may be expressed by

$$\begin{aligned}\sigma_{\widetilde{w}_r}^2 &= E\left[\sum_{m=1}^{M}\sum_{k=0}^{k=N-1}\left(c_r^{(m)}[k]\, w_r^{(m)}[n-k] - c_i^{(m)}[k]\, w_i^{(m)}[n-k]\right)\right.\\ &\quad\cdot \sum_{p=1}^{M}\sum_{kk=0}^{kk=N-1}\left(c_r^{(p)}[kk]\, w_r^{(p)}[n-kk]\right.\\ &\qquad\left.\left. - c_i^{(p)}[kk]\, w_i^{(p)}[n-kk]\right)\right]\end{aligned} \tag{9}$$

which can be written according to [6] as

$$\begin{aligned}\sigma_{\widetilde{w}_r}^2 &= \sum_{m=1}^{M}\sigma_{w_r}^2 \sum_{k=0}^{k=N-1}\left|c^{(m)}[k]\right|^2\\ &\quad + \sum_{m=1, m\neq p}^{M}\sum_{p=1, p\neq m}^{M}\frac{\sigma_{w_r}^2}{2}\left[\left(\left|m-p\right|-1\right)^{2H} - 2\left(\left|m-p\right|\right)^{2H}\right.\\ &\qquad\left. + \left(\left|m-p\right|+1\right)^{2H}\right]\\ &\quad\cdot \sum_{k=0}^{k=N-1}\left[c_r^{(m)}[k]\, c_r^{(p)}[k] + c_i^{(m)}[k]\, c_i^{(p)}[k]\right].\end{aligned} \tag{10}$$

This expression (10) was shown in [6] to be equal to (7) with the help of the triangle inequality [36], the Holder inequality [36], and the approximation given by [34]

$$0.5\left[\left(|m-p|-1\right)^{2H}-2\left(|m-p|\right)^{2H}+\left(|m-p|+1\right)^{2H}\right] \simeq H\left(2H-1\right)|m-p|^{2H-2}. \tag{11}$$

Next we turn to the expression for m_p. According to [1],

$$\begin{aligned} E\left[\Delta\left(p_r^2\right)\right] &= -2E\left[p_r\left(P_r\left[z\left[n\right]\right]\sum_{m=1}^{m=M}\mu^{(m)}\left\|\underline{y}^{(m)}\left[n\right]\right\|^2 + \Re\left(\sum_{m=1}^{m=M}\Delta_{(w*c)}^{(m)}\right)\right)\right] \\ &\quad + E\left[\left(-P_r\left[z\left[n\right]\right]\sum_{m=1}^{m=M}\mu^{(m)}\left\|\underline{y}^{(m)}\left[n\right]\right\|^2 - \Re\left(\sum_{m=1}^{m=M}\Delta_{(w*c)}^{(m)}\right)\right)^2\right], \end{aligned} \tag{12}$$

where $\Delta(p_r^2) = p_r^2[n+1] - p_r^2[n]$, $\Re(\cdot)$ is the real part of $(\cdot)$, $P_r[z[n]]$ is the real part of $P[z[n]]$, and $\Delta_{(w*c)}^{(m)} = w^{(m)}[n] * c^{(m)}[n+1] - w^{(m)}[n] * c^{(m)}[n] = w^{(m)} * (c^{(m)}[n+1] - c^{(m)}[n])$. By using (3) and (4), we may have for the nonblind case $P_r[z[n]] = p_r[n] + \widetilde{w}_r[n] = p_r + \widetilde{w}_r[n]$ (where $p_r = p_r[n]$). According to [1], when the equalizer has converged we have $\sum_{m=1}^{m=M}\Delta_{(w*c)}^{(m)} \to 0$ and $E[\Delta(p_r^2)] \cong 0$. Thus, after substituting $P_r[z[n]] = p_r + \widetilde{w}_r[n]$ and $E[\Delta(p_r^2)] = 0$ into (12) we obtain

$$\begin{aligned} &-2E\left[p_r\left(p_r+\widetilde{w}_r\left[n\right]\right)\right]\sum_{m=1}^{m=M}\mu^{(m)}E\left[\left\|\underline{y}^{(m)}\left[n\right]\right\|^2\right] \\ &\quad + E\left[\left(p_r+\widetilde{w}_r\left[n\right]\right)^2\right]E\left[\left(\sum_{m=1}^{m=M}\mu^{(m)}\left\|\underline{y}^{(m)}\left[n\right]\right\|^2\right)^2\right] \\ &= 0. \end{aligned} \tag{13}$$

According to [1], $E[(\|\underline{y}^{(m)}[n]\|^2)^2]$ may be approximated as $(E[\|\underline{y}^{(m)}[n]\|^2])^2$. Thus we obtain

$$\begin{aligned} &-2m_pE\left[\sum_{m=1}^{m=M}\mu^{(m)}\left\|\underline{y}^{(m)}\left[n\right]\right\|^2\right] \\ &\quad + \left(m_p+\sigma_{\widetilde{w}_r}^2\right)\left(E\left[\sum_{m=1}^{m=M}\mu^{(m)}\left\|\underline{y}^{(m)}\left[n\right]\right\|^2\right]\right)^2 = 0. \end{aligned} \tag{14}$$

From (14) we have

$$\begin{aligned} m_p &= \frac{\sigma_{\widetilde{w}_r}^2\left(E\left[\sum_{m=1}^{m=M}\mu^{(m)}\left\|\underline{y}^{(m)}\left[n\right]\right\|^2\right]\right)^2}{2E\left[\sum_{m=1}^{m=M}\mu^{(m)}\left\|\underline{y}^{(m)}\left[n\right]\right\|^2\right]-\left(E\left[\sum_{m=1}^{m=M}\mu^{(m)}\left\|\underline{y}^{(m)}\left[n\right]\right\|^2\right]\right)^2} \\ &= \frac{\sigma_{\widetilde{w}_r}^2\left(E\left[\sum_{m=1}^{m=M}\mu^{(m)}\left\|\underline{y}^{(m)}\left[n\right]\right\|^2\right]\right)}{2-\left(E\left[\sum_{m=1}^{m=M}\mu^{(m)}\left\|\underline{y}^{(m)}\left[n\right]\right\|^2\right]\right)}. \end{aligned} \tag{15}$$

Next we substitute [1] $E[\|\underline{y}^{(m)}[n]\|^2] = N\sigma_x^2(\sum_{k=0}^{k=R-1}|h_k^{(m)}[n]|^2 + (1/\mathrm{SNR}))$ into (15) and obtain the expression for m_p given in (6). This completes our proof. □

3.2. Derivation of the SER for the SIMO Case. In this subsection, we derive the SER for a source signal $x[n]$ belonging to a rectangular QAM constellation, applicable for the SIMO and fGn case.

Theorem 2. *Based on the assumptions given in the previous subsection, the SER for the nonblind adaptive version valid for the SIMO and fGn case may be defined as*

$$SER_{QAM} = 4\frac{\widetilde{M}-1}{\widetilde{M}}Q\left(\frac{d}{\sigma_T}\right)\left(1-\frac{\widetilde{M}-1}{\widetilde{M}}Q\left(\frac{d}{\sigma_T}\right)\right), \tag{16}$$

where $\widetilde{M} = \sqrt{M_{QAM}}$ and M_{QAM} is the number of signal points for a M_{QAM}-ary QAM constellation, d is half the distance between adjacent $\sqrt{M_{QAM}}$-ary PAM (pulse amplitude modulation) signals:

$$\sigma_T = \sqrt{m_p+\sigma_{\widetilde{w}_r}^2}; \qquad Q\left(\frac{d}{\sigma_T}\right) = \frac{1}{\sqrt{2\pi}}\int_{d/\sigma_T}^{\infty}e^{-u^2/2}du \tag{17}$$

and m_p, $\sigma_{\widetilde{w}_r}^2$ are according to (6) *and* (7)*, respectively.*

Proof. According to [6], the equalized output for the blind adaptive version for the SIMO case is given by $z[n] = x[n] + p[n] + \widetilde{w}[n]$. This expression is quite similar to the nonblind adaptive version given in (3). The difference between the two cases (blind and nonblind case) lies on the fact that the variance of $p[n]$ is very different. For each case, the expression for the variance of the real part of $p[n]$ (named in this paper as m_p) is different. However, the expression for the variance of the real part of $\widetilde{w}[n]$ (named in this paper as $\sigma_{\widetilde{w}_r}^2$) is the same for both cases. Recently [6], a closed-form approximated expression was obtained for the SER (blind adaptive version), based on $z[n] = x[n] + p[n] + \widetilde{w}[n]$, valid for the SIMO and fGn case where H is in the region of $0.5 \le H < 1$. The recently obtained expression for the SER [6] is recalled in (16) and (17). In order to obtain a closed-form approximated expression for the SER valid for the nonblind adaptive, SIMO and fGn case,

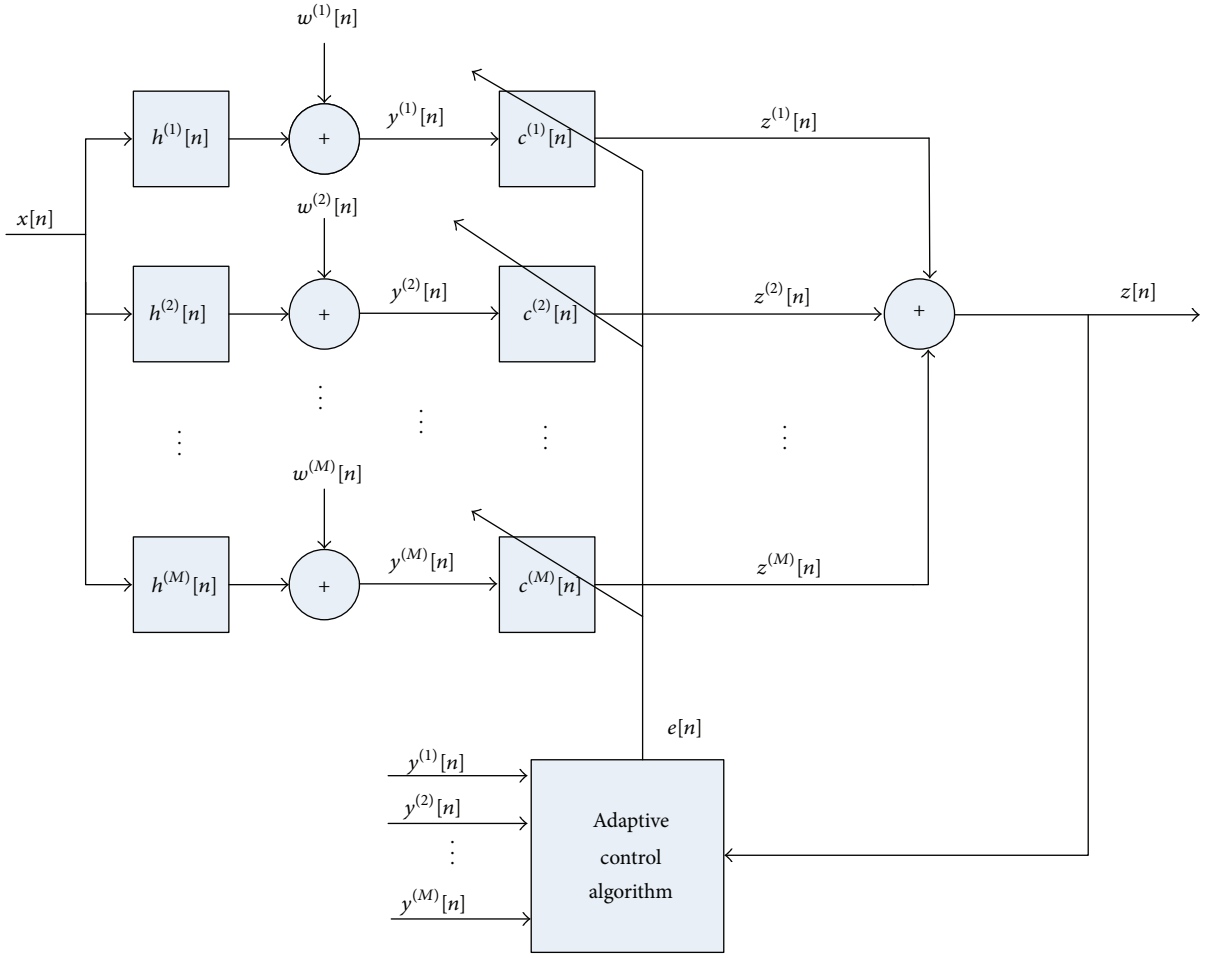

Figure 1: Block diagram of a baseband SIMO communication system.

the recently obtained expression for the SER [6] was used with m_p and $\sigma^2_{\widetilde{w}_r}$ ((6) and (7), resp.), valid for the nonblind adaptive, SIMO and fGn case. This completes our proof. □

4. Simulation

In this section we test our new proposed expression for the SER for the 16QAM case (a modulation using $\pm\{1, 3\}$ levels for in-phase and quadrature components) for different values of SNR and equalizer's tap length and for four different channel cases. The equalizer taps were updated according to (4) where we set for simplicity $\mu^{(m)} = \mu$. In the following we consider four channel cases:

channel case A which is a four-channel model with channel coefficients determined according to

$$\begin{aligned} h_1 &= \left[-0.0318 + j0.2330 \;\; 0.3128 - j0.3693 \;\; -0.3609 + j0.3810 \;\; 0.6490 \;\; -0.1110 + j0.0396\right], \\ h_2 &= \left[0.3005 - j0.0247 \;\; 0.6784 \;\; 0.6248 - j0.1316 \;\; 0.1282 - j0.1411 \;\; -0.0590 - j0.0366\right], \\ h_3 &= \left[-0.1351 - j0.2061 \;\; -0.1274 + j0.5876 \;\; 0.6401 \;\; -0.1818 - j0.3354 \;\; 0.0871 - j0.1216\right], \\ h_4 &= \left[0.2835 + j0.0204 \;\; 0.6799 \;\; 0.5936 + j0.0986 \;\; 0.1938 + j0.2101 \;\; -0.0333 + j0.1095\right] \end{aligned} \tag{18}$$

channel case B which is a two-channel model with channel coefficients determined according to

$$\begin{aligned} h_1 &= \left[-0.4000 \;\; 0.8000 \;\; 0.3200 \;\; 0.1280 \;\; 0.0512 \;\; 0.0205 \;\; 0.0082 \;\; 0.0033 \;\; 0.0013 \;\; 0.0005 \;\; 0.0002 \;\; 0.0001 \;\; 0.0000\right] \\ h_2 &= \left[1.3000 \;\; 0.6000 - j0.6364 \;\; 0 \;\; 0 \;\; 0 \;\; 0 \;\; 0 \;\; 0 \;\; 0 \;\; 0 \;\; 0 \;\; 0 \;\; 0\right]; \end{aligned} \tag{19}$$

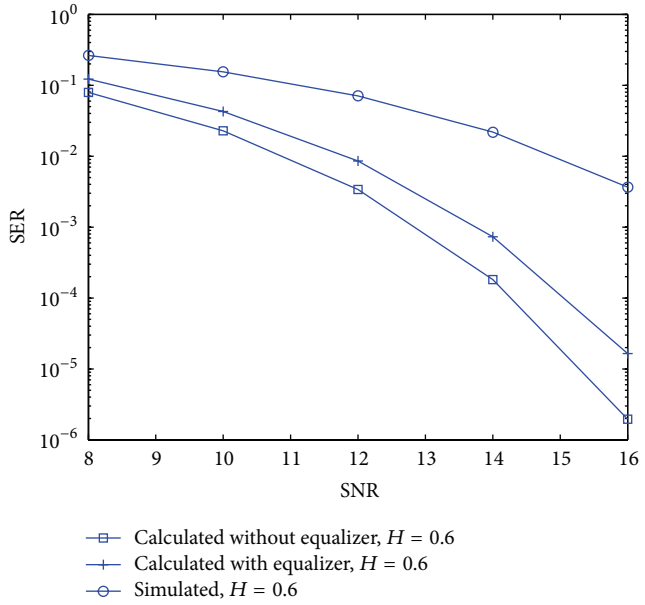

FIGURE 2: SER comparison with the following parameters: $d = 1$, the stepsize parameter $\mu = 0.0005$, $N = 17$, $H = 0.6$, and channel case A; the results were obtained for 1600000 symbols.

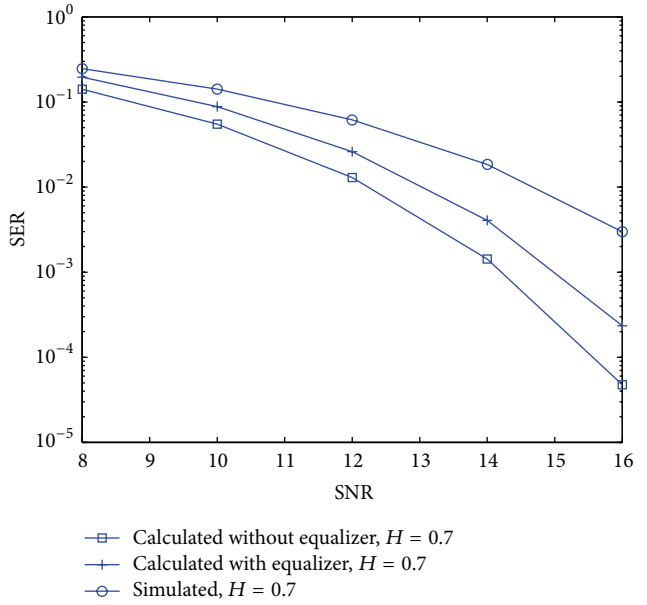

FIGURE 3: SER comparison with the following parameters: $d = 1$, the stepsize parameter $\mu = 0.0005$, $N = 17$, $H = 0.7$, and channel case A; the results were obtained for 1600000 symbols.

channel case C which is a four-channel model with complex channel coefficients. Each subchannel has a five-channel tap length with randomly generated complex coefficients at each time where no common zero among all the subchannels is generated;

channel case D which is a two-channel model with complex channel coefficients. Each subchannel has a three-channel tap-length with randomly generated complex coefficients at each time where no common zero among all the subchannels is generated.

Please note that channel cases A and B were also used in [6]. The equalizers were initialized by setting the center tap equal to one and all others to zero.

In the following we denote the SER performance according to (16) as "Calculated with Equalizer." In addition, we wish to show the SER performance for the case where the residual ISI is not taken into account. Therefore, we denote in the following the SER performance that does not take into account the residual ISI as "Calculated without Equalizer." Figure 2 to Figure 16 show the SER performance for different values of H and four channel cases as a function of SNR of our proposed expression (16) compared with the simulated results and with those calculated results that do not take into account the residual ISI. According to Figures 2, 3, 4, 6, 7, 10, 11, 12, 14, and 15 the calculated results (16) describe closer the simulated results in comparison to the results that do not take into account the residual ISI. According to Figures 5, 8, 9, 13, and 16 the proposed expression for the SER (16) may be considered only as the upper bound for the simulated results. According to Figure 10 to Figure 16, the proposed expression for the SER (16) for $H = 0.7$ is a very accurate approximation

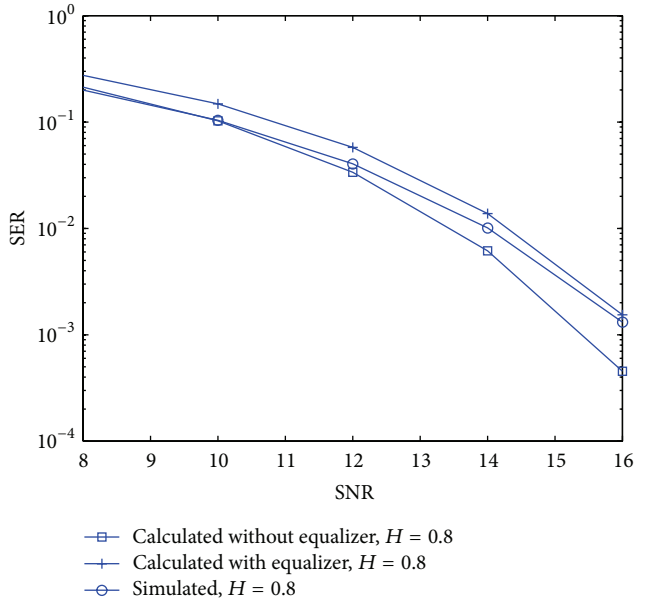

FIGURE 4: SER comparison with the following parameters: $d = 1$, the stepsize parameter $\mu = 0.0005$, $N = 17$, $H = 0.8$, and channel case A; the results were obtained for 1600000 symbols.

for the actual SER. Thus, the proposed expression for the SER (16) for $H = 0.7$ can be very useful for the system designer when dealing with time varying channels where the averaged SER is needed with high accuracy. But, if the averaged SER is not needed with such high accuracy for the time-varying channel case, then the proposed expression for the SER (16) is also very useful for the range of $0.6 \leq H < 0.7$ where it provides the system designer a more accurate approximation for the averaged SER compared to

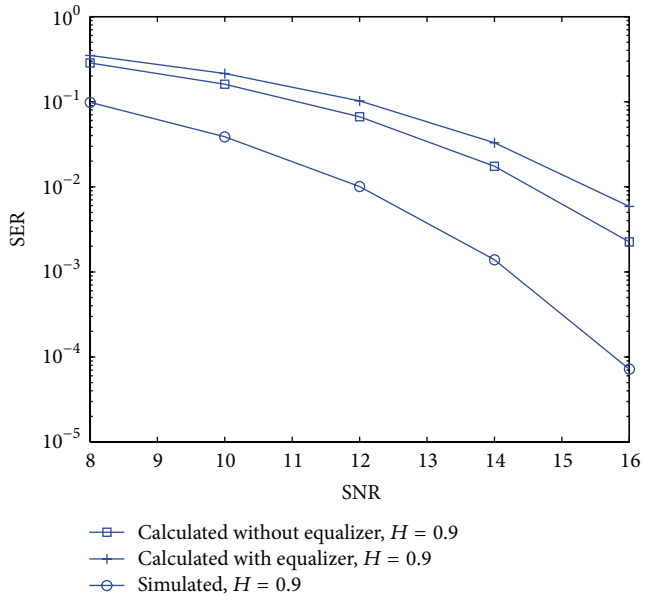

FIGURE 5: SER comparison with the following parameters: $d = 1$, the stepsize parameter $\mu = 0.0005$, $N = 17$, $H = 0.9$, and channel case A; the results were obtained for 1600000 symbols.

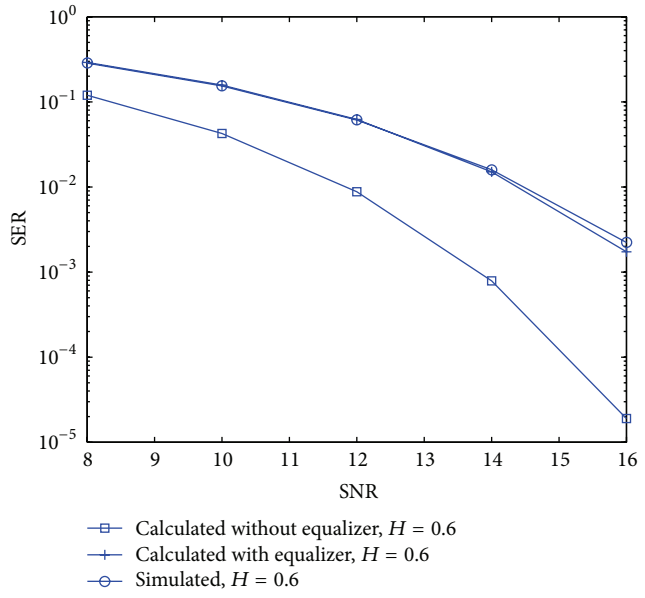

FIGURE 6: SER comparison with the following parameters: $d = 1$, the stepsize parameter $\mu = 0.002$, $N = 13$, $H = 0.6$, and channel case B; the results were obtained for 1600000 symbols.

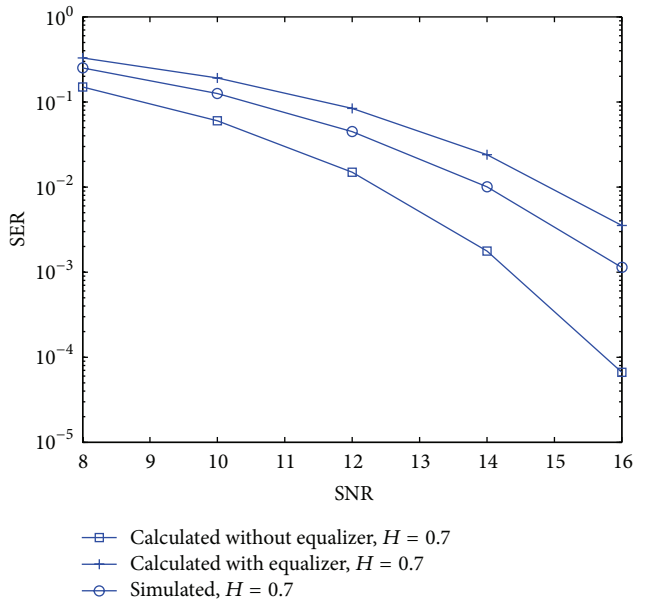

FIGURE 7: SER comparison with the following parameters: $d = 1$, the stepsize parameter $\mu = 0.002$, $N = 13$, $H = 0.7$, and channel case B; the results were obtained for 1600000 symbols.

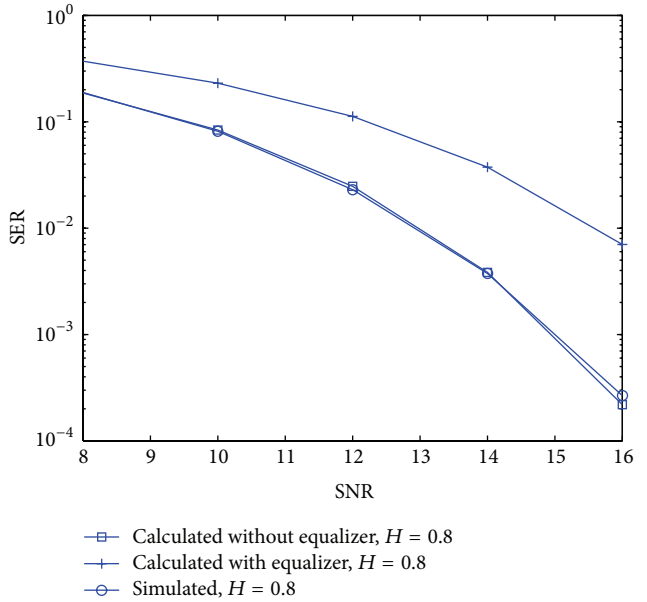

FIGURE 8: SER comparison with the following parameters: $d = 1$, the stepsize parameter $\mu = 0.002$, $N = 13$, $H = 0.8$, and channel case B; the results were obtained for 1600000 symbols.

the case where the expression for the SER is used that does not take into account the residual ISI. According to Figure 1, the equalized output $z[n]$ is the sum of the equalizer's output from each subchannel. For $H > 0.5$, the noise components from the different subchannels are dependent (please refer to assumption (4) in the system description section). In addition, according to (11), the noise dependency is stronger for higher values of H. Thus, it is reasonable to think that the SER might increase as the value for H increases due to the noise dependency from the different receiving paths. But, according to simulation results (Figure 2 to Figure 9), improved SER performance is seen for higher values of H. This outcome was also seen in [6]. The reason for having improved SER performance (Figure 2 to Figure 9) for higher

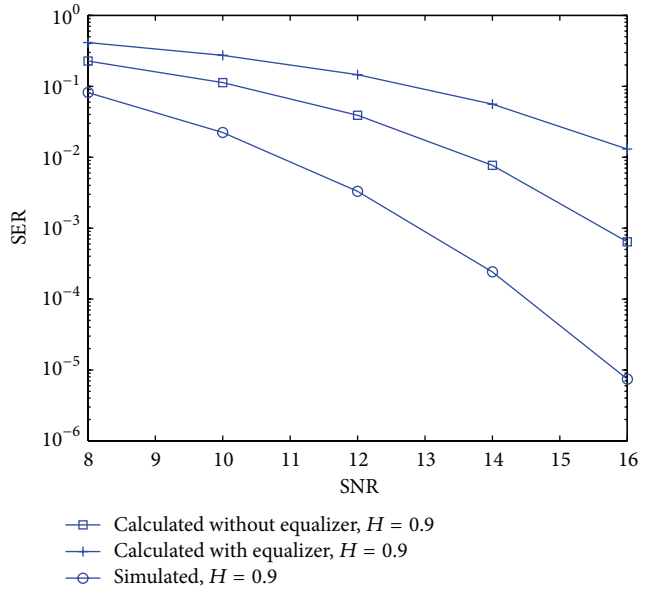

Figure 9: SER comparison with the following parameters: $d = 1$, the stepsize parameter $\mu = 0.002$, $N = 13$, $H = 0.9$, and channel case B; the results were obtained for 1600000 symbols.

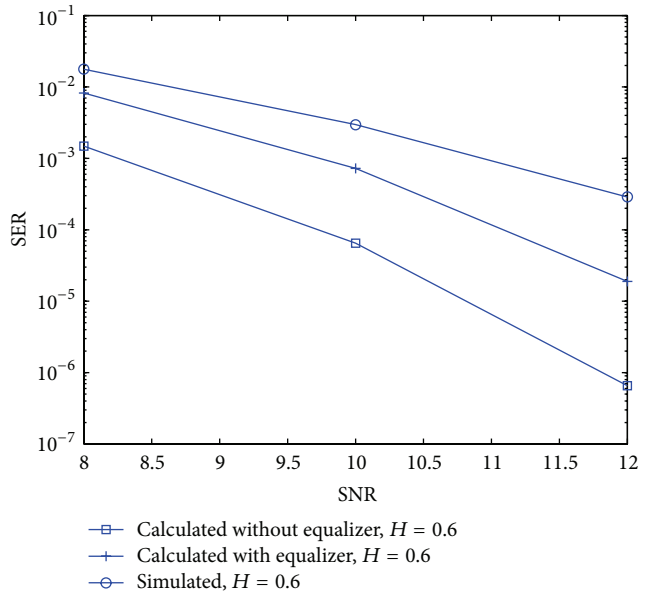

Figure 10: SER comparison with the following parameters: $d = 1$, the stepsize parameter $\mu = 0.0005$, $N = 9$, $H = 0.6$, and channel case C; the averaged results were obtained in 50 Monte Carlo trials for 128000 symbols.

values of H may be explained via (10). The second part of the right side of (10) defined by

$$\sum_{m=1,m\neq p}^{M}\sum_{p=1,p\neq m}^{M}\frac{\sigma_{w_r}^2}{2}\left[\left(|m-p|-1\right)^{2H}-2\left(|m-p|\right)^{2H}+\left(|m-p|+1\right)^{2H}\right]\cdot\sum_{k=0}^{k=N-1}\left[c_r^{(m)}[k]\,c_r^{(p)}[k]+c_i^{(m)}[k]\,c_i^{(p)}[k]\right] \quad (20)$$

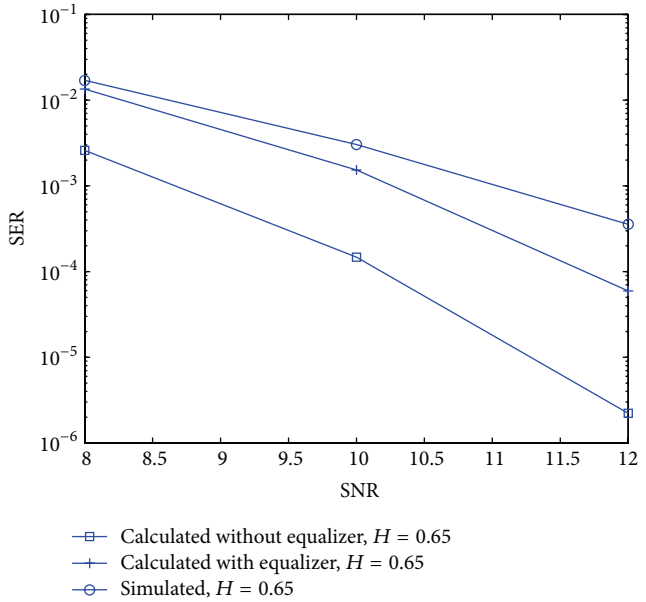

Figure 11: SER comparison with the following parameters: $d = 1$, the stepsize parameter $\mu = 0.0005$, $N = 9$, $H = 0.65$, and channel case C; the averaged results were obtained in 50 Monte Carlo trials for 128000 symbols.

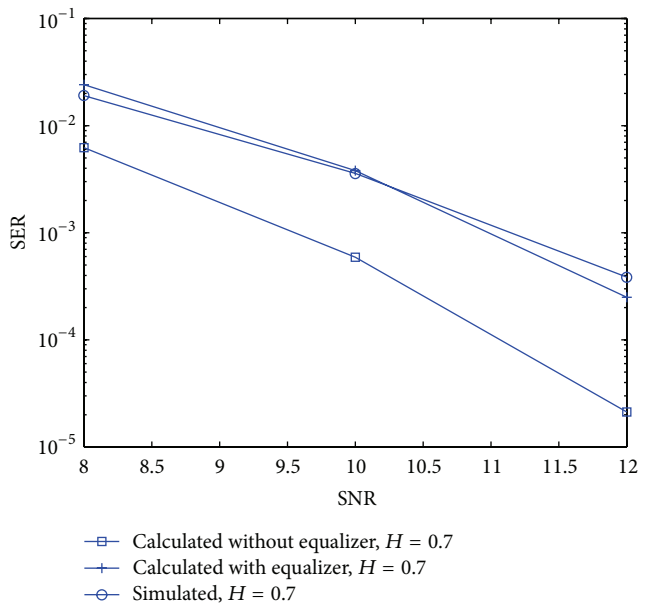

Figure 12: SER comparison with the following parameters: $d = 1$, the stepsize parameter $\mu = 0.0005$, $N = 9$, $H = 0.7$, and channel case C; the averaged results were obtained in 50 Monte Carlo trials for 128000 symbols.

can obtain negative values via $\sum_{k=0}^{k=N-1}[c_r^{(m)}[k]c_r^{(p)}[k] + c_i^{(m)}[k]c_i^{(p)}[k]]$. By using the approximation of (11) in (20), we can see that, for certain cases where $\sum_{k=0}^{k=N-1}[c_r^{(m)}[k]c_r^{(p)}[k] + c_i^{(m)}[k]c_i^{(p)}[k]]$ achieves a negative value, this negative value is multiplied by a positive value depending on H ($H(2H-1)|m-p|^{2H-2}$). Thus, for higher values of H and for the

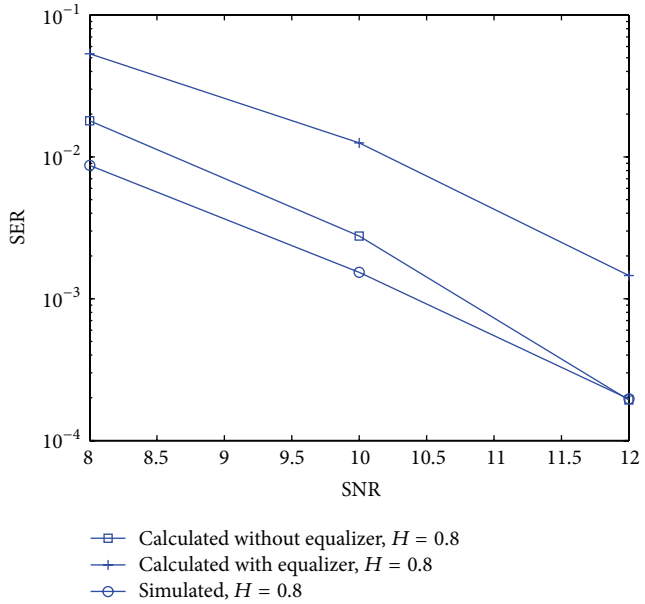

Figure 13: SER comparison with the following parameters: $d = 1$, the stepsize parameter $\mu = 0.0005$, $N = 9$, $H = 0.8$, and channel case C; the averaged results were obtained in 50 Monte Carlo trials for 128000 symbols.

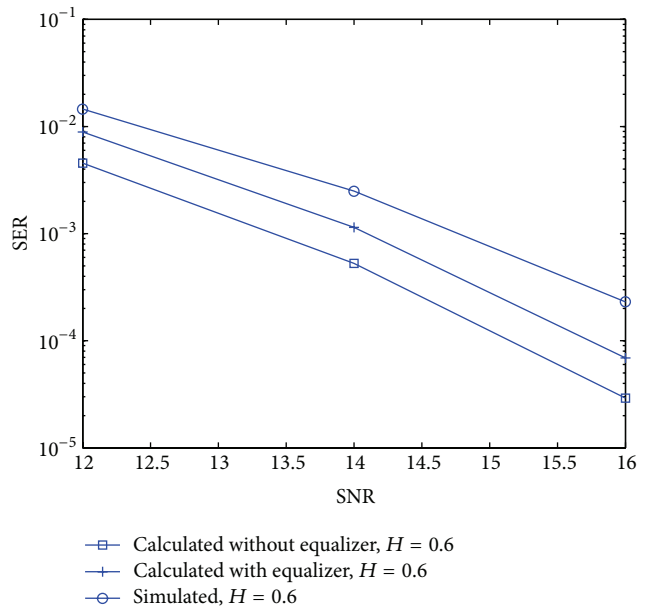

Figure 14: SER comparison with the following parameters: $d = 1$, the stepsize parameter $\mu = 0.0005$, $N = 19$, $H = 0.6$, and channel case D; the averaged results were obtained in 50 Monte Carlo trials for 128000 symbols.

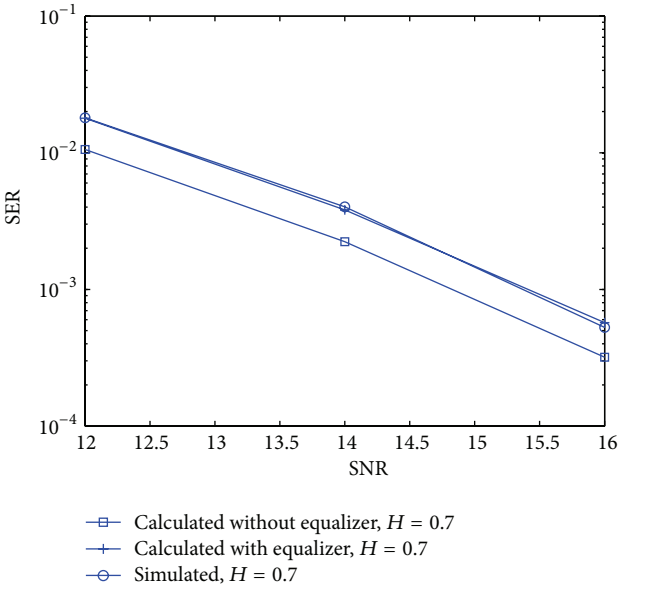

Figure 15: SER comparison with the following parameters: $d = 1$, the stepsize parameter $\mu = 0.0005$, $N = 19$, $H = 0.7$, and channel case D; the averaged results were obtained in 50 Monte Carlo trials for 128000 symbols.

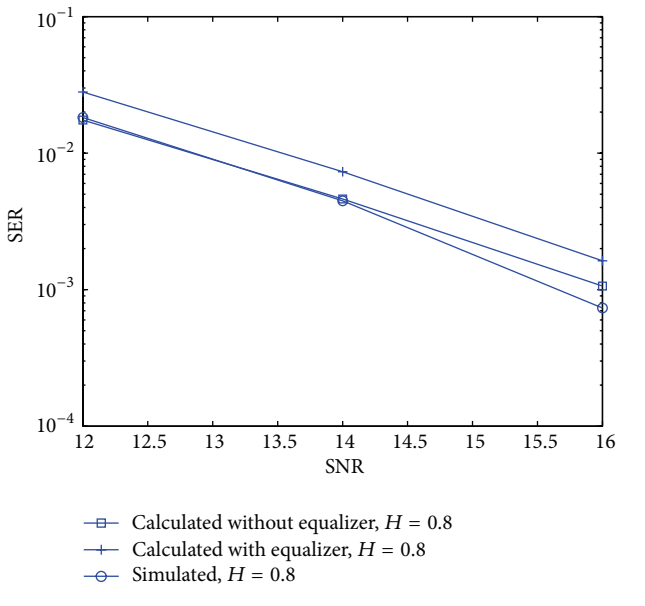

Figure 16: SER comparison with the following parameters: $d = 1$, the stepsize parameter $\mu = 0.0005$, $N = 19$, $H = 0.8$, and channel case D; the averaged results were obtained in 50 Monte Carlo trials for 128000 symbols.

case where $\sum_{k=0}^{k=N-1}[c_r^{(m)}[k]c_r^{(p)}[k] + c_i^{(m)}[k]c_i^{(p)}[k]] < 0$, $\sigma_{\widetilde{w}_r}^2$ (10) decreases which causes σ_T (17) to decrease which leads to improved SER. Since the equalizer's coefficients $c_r^{(m)}[k]$, $c_r^{(p)}[k]$, $c_i^{(m)}[k]$, and $c_i^{(p)}[k]$ are not available to us, $\sum_{k=0}^{k=N-1}[c_r^{(m)}[k]c_r^{(p)}[k] + c_i^{(m)}[k]c_i^{(p)}[k]]$ was upper limited (please refer for more details to [6]) in order to supply the system designer an expression for $\sigma_{\widetilde{w}_r}^2$ depending only on available parameters to him. Thus, the outcome was that $\sigma_{\widetilde{w}_r}^2$ as appears in (7) increases for higher values for H for all cases of $\sum_{k=0}^{k=N-1}[c_r^{(m)}[k]c_r^{(p)}[k] + c_i^{(m)}[k]c_i^{(p)}[k]]$, namely, also for the case where $\sum_{k=0}^{k=N-1}[c_r^{(m)}[k]c_r^{(p)}[k] + c_i^{(m)}[k]c_i^{(p)}[k]] < 0$. Thus,

the accuracy of our proposed expression for the SER (16) is dependent on H.

5. Conclusion

In this paper, we proposed for the real and two independent quadrature carrier case, closed-form approximated expressions for the residual ISI and SER obtained by nonblind adaptive equalizers that are applicable for the SIMO and fGn ($0.5 \leq H < 1$) input case. The expression for the SER depends on the system's parameters (stepsize parameter, equalizer's tap length, input constellation statistics, channel power, number of receiving antennas used in the SIMO system and on H). Thus, there is no need anymore to carry out any simulation in order to find those system's parameters that will lead to the required SER performance. According to simulation results, the proposed expression for the SER can be very useful for the system designer when dealing with time-varying channels where the averaged SER is needed and $H \leq 0.7$. For channel case A and $0.6 \leq H \leq 0.8$ or channel case B and $0.6 \leq H \leq 0.7$ the proposed expression for the SER provides better results for the simulated results in comparison to the results that do not take into account the residual ISI. For channel case A and $1 > H > 0.8$ or channel cases B, C, and D and $1 > H > 0.7$ the new proposed expression for the SER may be considered only as the upper bound for the simulated results. FGn with $H \in (0.5, 1)$ corresponds to the case of LRD. Thus, it could be thought that the SER might increase as the value for H increases due to the noise dependency from the different receiving paths. But, according to simulation results, improved SER performance is seen for higher values of H.

Conflict of Interests

The author declares that there is no conflict of interests regarding the publication of this paper.

Acknowledgment

The author would like to thank the reviewers for their helpful comments.

References

[1] M. Pinchas, "A closed-form approximated expression for the achievable residual ISI obtained by blind adaptive equalizers in a SIMO FIR channel," in *Proceedings of the 2012 IEEE 27th Convention of Electrical and Electronics Engineers in Israel*, Eilat, Israel, November 2012.

[2] I. Moazzen, A. M. Doost-Hoseini, and M. J. Omidi, "A novel blind frequency domain equalizer for SIMO systems," in *Proceedings of the International Conference on Wireless Communications and Signal Processing (WCSP '09)*, pp. 1–6, November 2009.

[3] D. Peng, Y. Xiang, Z. Yi, and S. Yu, "CM-based blind equalization of time-varying SIMO-FIR channel with single pulsation estimation," *IEEE Transactions on Vehicular Technology*, vol. 60, no. 5, pp. 2410–2415, 2011.

[4] A. Coskun and I. Kale, "Blind multidimensional matched filtering techniques for single input multiple output communications," *IEEE Transactions on Instrumentation and Measurement*, vol. 59, no. 5, pp. 1056–1064, 2010.

[5] S. van Vaerenbergh, J. Vía, and I. Santamaria, "Blind identification of SIMO Wiener systems based on kernel canonical correlation analysis," *IEEE Transactions on Signal Processing*, vol. 61, no. 9, pp. 2219–2230, 2013.

[6] M. Pinchas, "Symbol error rate as a function of the residual ISI obtained by blind adaptive equalizers for the SIMO and fractional Gaussian noise case," *Mathematical Problems in Engineering*, vol. 2013, Article ID 860389, 9 pages, 2013.

[7] http://books.google.co.il/books?id=bimBH2czOZ0C.

[8] S. Chen, A. Wolfgang, and L. Hanzo, "Constant modulus algorithm aided soft decision directed scheme for blind space-time equalisation of SIMO channels," *Signal Processing*, vol. 87, no. 11, pp. 2587–2599, 2007.

[9] D. Peng, Y. Xiang, H. Trinh, and Z. Man, "Adaptive blind equalization of time-varying SIMO systems driven by QPSK inputs," *Digital Signal Processing*, vol. 23, no. 1, pp. 268–274, 2013.

[10] D. Peng, Y. Xiang, and D. Huang, "Estimation of basis frequencies for time-varying SIMO channels: a second-order method," *IEEE Transactions on Signal Processing*, vol. 58, no. 8, pp. 4026–4039, 2010.

[11] K. I. Diamantaras and T. Papadimitriou, "An efficient subspace method for the blind identification of multichannel FIR systems," *IEEE Transactions on Signal Processing*, vol. 56, no. 12, pp. 5833–5839, 2008.

[12] S. Wang, J. Manton, D. B. H. Tay, C. Zhang, and J. C. Devlin, "An FFT-based method for blind identification of FIR SIMO channels," *IEEE Signal Processing Letters*, vol. 14, no. 7, pp. 437–440, 2007.

[13] N. Gu, Y. Xiang, M. Tan, and Z. Cao, "A new blind-equalization algorithm for an FIR SIMO system driven by MPSK signal," *IEEE Transactions on Circuits and Systems II*, vol. 54, no. 3, pp. 227–231, 2007.

[14] M. Reuter and J. R. Zeidler, "Nonlinear effects in LMS adaptive equalizers," *IEEE Transactions on Signal Processing*, vol. 47, no. 6, pp. 1570–1579, 1999.

[15] A. H. I. Makki, A. K. Dey, and M. A. Khan, "Comparative study on LMS and CMA channel equalization," in *Proceedings of the International Conference on Information Society (i-Society '10)*, pp. 487–489, June 2010.

[16] E. Tucu, F. Akir, and A. Zen, "A new step size control technique for blind and non-blind equalization algorithms," *Radioengineering*, vol. 22, no. 1, p. 44, 2013.

[17] http://www.academypublisher.com/proc/iscsct10/papers/iscsct10p256.pdf.

[18] M. Pinchas, *The Whole Story Behind Blind Adaptive Equalizers/Blind Deconvolution*, e-books Publications Department, Bentham Science Publishers, 2012.

[19] M. Pinchas, "Residual ISI obtained by nonblind adaptive equalizers and fractional noise," *Mathematical Problems in Engineering*, vol. 2013, Article ID 830517, 7 pages, 2013.

[20] J. Beran, *Statistics for Long-Memory Processes*, Chapman and Hall, New York, NY, USA, 1994.

[21] M. Li and W. Zhao, "On $1/f$ noise," *Mathematical Problems in Engineering*, vol. 2012, Article ID 673648, 23 pages, 2012.

[22] M. Li, "Fractal time series—a tutorial review," *Mathematical Problems in Engineering*, vol. 2010, Article ID 157264, 26 pages, 2010.

[23] M. Li and W. Zhao, "Quantitatively investigating locally weak stationarity of modified multifractional Gaussian noise," *Physica A*, vol. 391, no. 24, pp. 6268–6278, 2012.

[24] http://www.bearcave.com/misl/misltech/wavelets/hurst/.

[25] J. Alvarez-Ramirez, J. C. Echeverria, and E. Rodriguez, "Performance of a high-dimensional R/S method for Hurst exponent estimation," *Physica A*, vol. 387, no. 26, pp. 6452–6462, 2008.

[26] G. Malik and A. S. Sappal, "Adaptive equalization algorithms: an overview," *International Journal of Advanced Computer Science and Applications*, vol. 2, no. 3, pp. 62–67, 2011.

[27] M. Pinchas, *Blind Equalizers by Techniques of Optimal Non-Linear Filtering Theory*, VDM Verlagsservice gesellschaft mbH, 2009.

[28] M. Pinchas and B. Z. Bobrovsky, "A maximum entropy approach for blind deconvolution," *Signal Processing*, vol. 86, no. 10, pp. 2913–2931, 2006.

[29] M. Pinchas and B. Z. Bobrovsky, "A novel HOS approach for blind channel equalization," *IEEE Transactions on Wireless Communications*, vol. 6, no. 3, pp. 875–886, 2007.

[30] C. L. Nikias and A. P. Petropulu, Eds., *Higher-Order Spectra Analysis a Nonlinear Signal Processing Framework*, pp. 419–425, chapter 9, Prentice-Hall, 1993.

[31] S. Haykin, "Blind deconvolution," in *Adaptive Filter Theory*, S. Haykin, Ed., chapter 20, Prentice-Hall, Englewood Cliffs, NJ, USA, 1991.

[32] S. Fiori, "A contribution to (neuromorphic) blind deconvolution by flexible approximated Bayesian estimation," *Signal Processing*, vol. 81, no. 10, pp. 2131–2153, 2001.

[33] S. Bellini, "Bussgang techniques for blind equalization," in *Proceedings of the IEEE Global Telecommunication Conference Records*, pp. 1634–1640, December 1986.

[34] M. Li and W. Zhao, "On bandlimitedness and lag-limitedness of fractional Gaussian noise," *Physica A*, vol. 392, no. 9, pp. 1955–1961, 2013.

[35] M. Li, "Fractional Gaussian noise and network traffic modeling," in *Proceedings of the 8th WSEAS International Conference on Applied Computer and Applied Computational Science*, Hangzhou, China, May 2009.

[36] M. R. Spiegel, *Mathematical Handbook of Formulas and Tables*, SCHAUM's Outline Series, McGraw-Hill, New York, NY, USA, 1968.